



Decolorization of the aqueous Safranin O dye solution using *Thuja orientalis* as biosorbent.

Dunya Edan Al- Mammar*

Department of Chemistry, College of Science, University of Baghdad, Baghdad, Iraq.

Abstract

The object of this study was to evaluate the efficiency of safranin O (SFO), dye removal with application of *Thuja orientalis* as a low-cost biosorbent. The biosorption equilibrium level was determined as a function of pH, adsorbent dose, contact time and temperature. Surface area and pore size distribution were measured for the adsorbent. *Thuja* has a good removal efficiency for SFO dye. The adsorption kinetics data were best fit for the pseudo-second order kinetic (the regression coefficient = 0.999). The experimental equilibrium adsorption data are tested for the Langmuir, freundlich, Temkin and Dubinin-Radushkevich isotherm models. From the values of the regression coefficient the results indicate the following order to fit the isotherm Freundlich > Temkin > Dubinin-Radushkevich > Langmuir. A chemical adsorption process was indicated by the value of the mean free energy of adsorption obtained from the Dubinin-Radushkevich isotherm. Standard free energy of adsorption (ΔG°) and the change in the standard enthalpy (ΔH°) and the standard entropy (ΔS°) were calculated to predict the nature of adsorption.

Keywords: Isotherm, Kinetic, Removal, Safranin O, *Thuja*.

إزالة اللون لمحاليل صبغة السفرائين (O) المائية باستخدام العفص الشرقي كمادة حيوية مازة

دنيا عيدان المعمار*

قسم الكيمياء، كلية العلوم، جامعة بغداد، بغداد، العراق.

الخلاصة:

يتضمن موضوع الدراسة تخمين كفاءة ثمرة العفص الشرقي في إزالة صبغة السفرائين (O) كمادة نباتية مازة رخيصة. تم تعيين مستوى الامتزاز المتوازن كدالة لجرعات المادة المازة، الدالة الحامضية، زمن التماس، ودرجة الحرارة. وتم قياس المساحة السطحية وتوزيع مقاسات المسام للمادة المازة. لثمرة العفص كفاءة جيدة لإزالة صبغة السفرائين (O). معلومات حركيات الامتزاز تتطابق بصورة جيدة مع سرعة تفاعل المرتبة الثانية المنتحلة (معامل التصحيح = 0.999). ان نتائج تجارب الامتزاز المتوازنة تم اختبارها على نماذج متساوي درجة الحرارة لنكماير، فرنديش، تمكين، ودوين رادشكفج. من قيم معامل التصحيح يظهر ان النتائج تتبع الترتيب فرنديش < تمكين < دوين رادشكفج < لنكماير. عملية امتزاز كيميائي ويمكن الاستدلال عليها من قيمة طاقة الامتزاز من ايزوثيرم دوين رادشكفج. الطاقة الحرة القياسية للامتزاز، التغير في الانتالبي القياسي، والتغير في الانتروبي القياسي تم حسابهم لمعرفة طبيعة الامتزاز.

*Email: dn_almammar@yahoo.com

I. Introduction

In the textile industry, one of the main problems is the removal of dyes and pigments from the wastewaters. The discharge of dye-bearing wastewater into natural streams and rivers poses a serious pollution problem, as dyes impart toxicity to aquatic life and are damaging the aesthetic nature of the environment [1, 2]

Safranin O is a water soluble phenazine dye (3, 7-diamino-2, 8-dimethyl-5 phenyl-phenazinium chloride), $C_{20}H_{19}N_4Cl$, reddish brown powder. The structure of SFO is given in Figure 1. This dye is a biological stain used in histology and cytology [3]. It is commonly used for staining gram negative bacteria red in smears to contrast with the blue gram positive organisms. It can also be used for the detection of the cartilage, mucin and mast cell granules. This dye also used for dyeing tannin, cotton, bast fibers, wool, silk, leather and paper.

Dye residues are esthetically unpleasant and interfere with the transmission of light necessary to photosynthesis, causing disturbance in the ecological systems of the receiving water. Although contaminated wastewater may be treated with conventional physical-chemical process such as membrane filtration, reverse osmosis [4], ion exchange, chemical oxidation, electro-flotation, electro-kintic coagulation [5] and irradiation, the application of these techniques has been restricted due to high energy consumption or expensive synthetic resins and chemicals [6]. Moreover, these methods generate large amount of toxic sludge and are ineffective at lower concentration of dye. Therefore development innovative, but low cost processes by which dye molecules can be removed [7]. Research is therefore need to develop a new alternative environmental friendly application.

The adsorption process give the best results as they can be used to remove different types of coloring materials, providing an alternative treatment especially if "low cost" adsorbent are available. Recently, a number of low-cost adsorbent for dye removal from mineral wastes [8], agricultural wastes, microbial biomass [9] and higher plant biomass were reported in literature. Among them biomaterials from higher plants seem to be one type of popular low-cost adsorbents because they usually have higher biomass compared with microbes and easily available. For example, tree fern [10], orange peel [11], date pits [12], peanut hull [13], phoenix tree leaves [14] and plam kernel fiber [15].

According to literature survey, recently activated carbon and activated rice husk [16] and micellar enhanced ultrafiltration [17] were used to remove safranin O from waste water. Thuja orientalis are readily available biosorbents in nature [18]. Their trees belong to cupressaceae (capress family). The aim of this study was to clarify adsorption behavior of Thuja biomass for decolorization of the wastewater. The data have been obtained for kinetic, thermodynamic and equilibrium situation. Four equilibrium isotherm models were applied to help the description of the adsorption process.

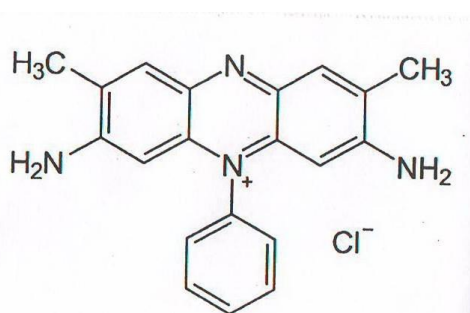


Figure 1- The Molecular structure of Safranin O

II. Experimental

2.1 Materials

2.1.1 Biosorbent preparation:

Thuja orientalis [from south of Iraq- Dhoke] were used in this investigation. Thuja were collected in July of 2012. Fresh Thuja biosorbent were dried at 90°C for 48h and cut into small pieces, ground in a mortar to powder.

2.1.2 Preparation of Safranin O Solution:

Safranin O (M.W= 350.85 g.mol⁻¹) cationic dye, was provided by Fluka. A stock standard solution of SFO dye at concentration of 100 mg L⁻¹ was prepared by dissolving 100mg in 1000ml distilled water, then (5,10,15,20,25)mg from the stock solution was dissolved in 1000ml distilled water for the preparation of other concentrations from the dye solution.

2.2 Apparatus:

All of spectrophotometric measurement of the dye was done at its λ_{max} (520 nm) [17] by UV –Vis spectrophotometer (UV-1800 shimadzu, Japan). The pH meter (HANNA, model 211, England) was used in the pH measurements. A GRIFEN FLASK SHAKER (London) was applied for shaking of the dye solutions. Surface area was determined by using surface area analyzer type (SA- 2900 HORIBA, USA). Pore diameter and pore size distribution were measured using Atomic force microscopy (AFM, type AA3000, Angstrom). FT-IR spectra was obtained using Shimadzu, model FTIR-8400.

2.3 Batch adsorption studies: The adsorption of SFO into adsorbent was investigated in batch experiments.

2.3.1 Effect of initial solution pH:

The effect of pH on dye SFO was evaluated by adding 0.25g of adsorbent into flasks containing 50ml of 20mg L⁻¹ SFO solutions at different initial pH (1-12). The pH of solutions was adjusted using 0.1M HCl or NaOH. The adsorbent was added after SFO solution pH was fixed. Flasks containing the adsorbent and SFO solution were shaken at 150 rpm and 20°C for 60 min, initial and equilibrium pH of solutions SFO concentrations were measured.

2.3.2 Effect of adsorbent dosage:

Effect of adsorbent dosage was studied by adding different adsorbent doses (0.1-0.6g) into flasks containing 50 ml of 20 mg L⁻¹ SFO solutions. The pH of the solutions was preadjusted to 7. Flasks were shaken at 150 rpm and 20°C for 60 min, initial and equilibrium pH of solution and residual dye concentration in solution were measured.

2.3.3 Effect of contact time and temperature:

The influence of contact time and temperature on dye adsorption was studied at 20°C and 30°C with initial dye concentration 20 mg/L and adsorbent dose of 0.125 gm/25ml of solution

2.4 Kinetic study:

For sorption experiment, 0.25g of adsorbent was added to flasks containing 50 ml of 20 mg L⁻¹ SFO-bearing solution with pH adjusted to 7. Flasks were shaken at 150 rpm and 20°C. Aliquot amounts of solution were taken, periodically. Residual SFO concentration in solutions was measured.

2.5 Isothermal and thermodynamic study:

For isotherm analysis, adsorption experiments were conducted by varying the initial SFO concentration from 5mg L⁻¹ to 25 mg L⁻¹. 0.125gm of biosorbent was added to flasks containing 25ml of SFO-bearing solution with pH adjusted to 7. Flasks were shaken at 150 rpm at temperature range 10°C-40°C for 60 min. After equilibration, the remaining dye in solution was determined.

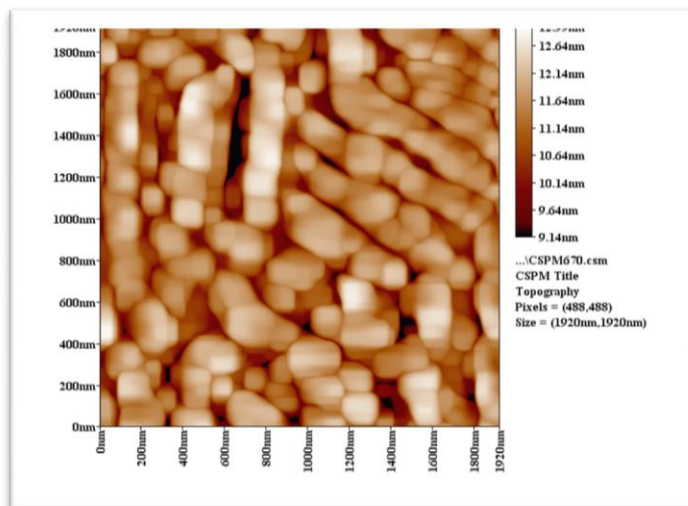
2.6 Conductivity measurement:

Conductivity is a measure of the ability of an aqueous solution to carry an electric current. This ability depends on the presence of ions on their total concentration, mobility, and valence. The conductivity of 1% solution of the biosorbent was determined using HANNA, model 99301 conductivity meter. The value of electrical conductivity was (1.33 ms/cm). The result obtained showed higher values of conductivity of the adsorbent than activated carbon [19] that could be attributed to a high content of dissolved ions and polar compounds.

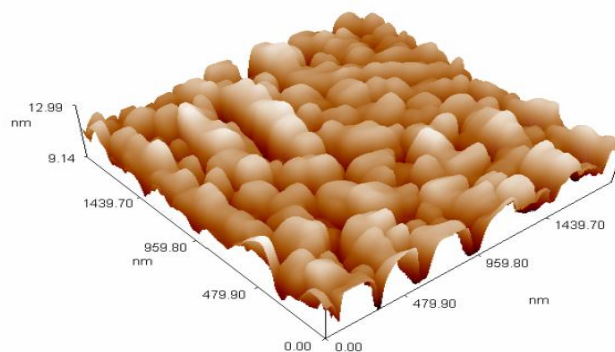
III. Results and discussion:

3.1 Surface area and pore size distribution:

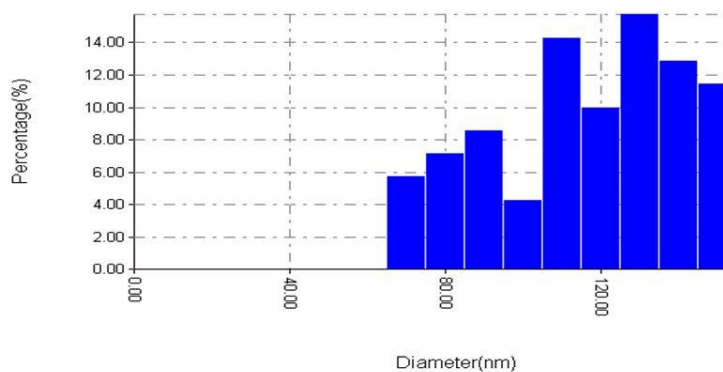
the value of surface area measured was found 27.7 m²/g, Figure 2 shows the surface morphology of the biosorbent. The microstructure of biosorbent image showed that the surface could be seen to contain amounts of pores; average pore size is equal to 116.29nm indicating that this material presents good characteristics to be employed as adsorbent for dye uptake. It is believed that these pores provide a ready access and large surface area for the sorption of dyes on the binding sites [20].



(A)



(B)



(C)

Figure 2- AFM images of Thuja: (A) the 2D, cross section. (B) 3D (C) Pore size distribution diagram

3.2 FT-IR measurement:

The infrared spectrum of Thuja (Figure 3) was tested using KBr technique. This measurement showed the presence of the following groups: $-\text{OH}$ and/or $-\text{NH}_2$ (3346.27 cm^{-1}) broadband, $-\text{CH}$ aliphatic (2665 cm^{-1}), $\text{C}=\text{O}$ at (1708 cm^{-1}), $\text{C}=\text{C}$ double bond at (1612 cm^{-1}), $-\text{NH}$ (1535.23 cm^{-1}), $\text{C}-\text{O}-\text{C}$ (1078.13 cm^{-1} and 1029.92 cm^{-1}), $\text{C}-\text{O}$ or $-\text{COOH}$ (1448.14 cm^{-1}) and $-\text{OCH}_3$ (1195.78 cm^{-1}).

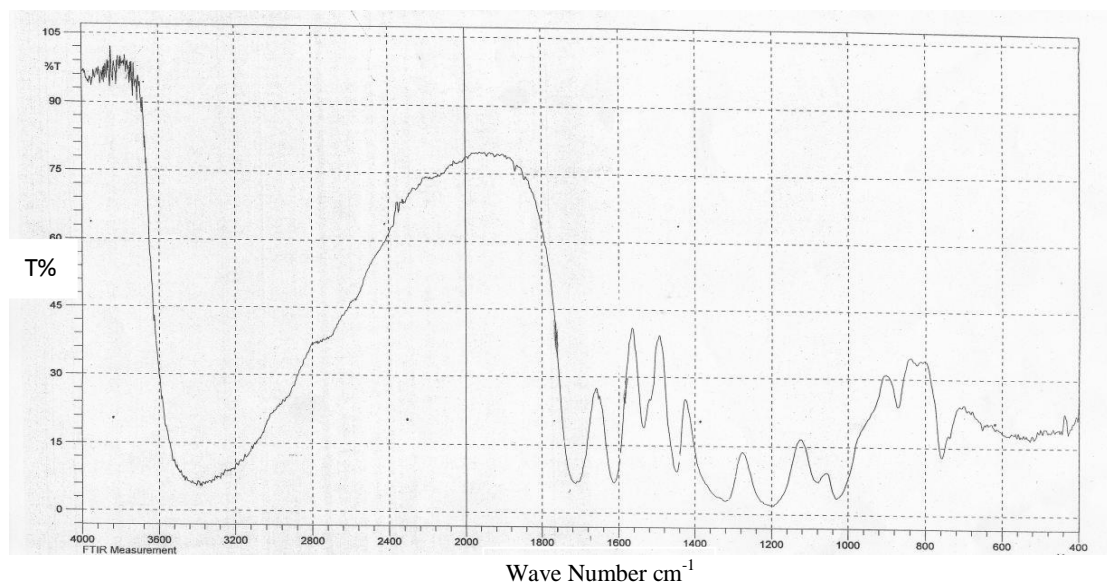


Figure 3- FT-IR of the Thuja biosorbent

3.3 Batch adsorption studies

3.3.1 Effect of pH:

Solution pH would affect both aqueous chemistry and surface binding-sites of the adsorbents and ionization/ dissociation of the adsorbate molecule. The effect of pH on the adsorption of SFO onto biosorbent at pH ranging 1 and 13 is shown in Figure 4. The removal percentage increased from 62% to 89.3% with increasing the initial pH from 1-12.

It can be seen that dye adsorption was unfavorable at $\text{pH} < 3$. The decrease in the adsorption with decrease in pH may be attributed to two reasons. As pH of the system decreased, the number of negatively charged adsorbent sites decreased and the number of positively charged surface sites increased, which did not favour the adsorption of positively charged dye cations due to electrostatic repulsion. Secondly, at lower pH, H^+ may compete with the dye cations for the adsorption sites of the Thuja biomass, thereby inhibiting the adsorption of the dyes [21]. As pH increased the biosorbent surface become more and more negatively charged and therefore the biosorption of cationic dye species were more favorable. So the best removal noticed at pH range from 7-12.

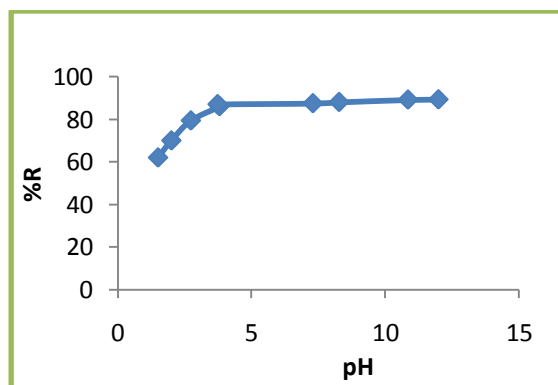


Figure 4- Effect of initial pH on SFO removal by the Thuja biosorbent.

3.3.2 Effect of adsorbent dosage on biosorption:

It is evident from Figure 5 that the sorption capacity of biosorbent decreased as adsorbent dose interferes between the binding sites and caused electrostatic interaction between cells. Adsorbent dose added into the solution determines the number of binding site available. An increase in adsorbent quantities strongly affects the quantities of dye removed from aqueous solution to certain limit [22]. The decrease in the sorption capacity may be attributed to the splitting effect of flux (concentration

gradient) between sorbate and adsorbent, with increasing adsorbent concentration causing a decrease in the amount of dye adsorbed onto unit weight of adsorbent.

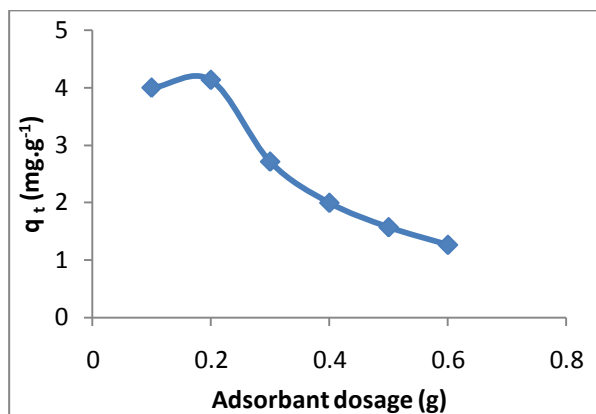


Figure 5- Effect of adsorbent dosage on SFO uptake using Thuja biomass.

3.3.3 Effect of contact time:

Figure 6 shows the effect of contact time on the adsorption of SFO on Thuja biomass. The equilibrium adsorption percent increases with increasing the contact time and approaches to equilibrium after about 50 min. therefore 60 min was accepted as optimal time for adsorption of SFO on the Thuja biomass because further increase in contact time did not show an increasing in biosorption. Initially a large number of vacant surface sites is available for adsorption; the adsorption rate is very fast, thus it rapidly increases the amount of adsorbates accumulated on the adsorbent surface mainly within the first hour of adsorption. As a result, the remaining vacant surface sites are difficult to be occupied due to the formation of repulsive forces between the dye molecular on the solid and the bulk phase [23].

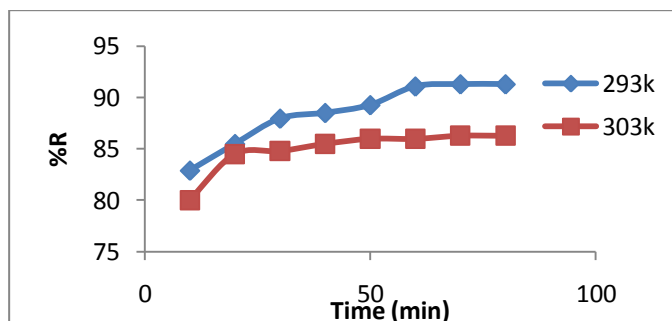


Figure 6- Effect of contact time and temperature on equilibrium adsorption of SFO onto Thuja biosorbent.

3.3.4 Effect of temperature:

Figure 6 shows the sorption of SFO removed at 293 and 303k at initial dye concentration of 20 mg L⁻¹. When increasing the temperature from 293 to 303k, the removal of the dye decreased from 91% to 86%. This may be due to a tendency for the dye molecules to escape from the solid phase to the bulk phase with an increase in temperature of the solution [24]. Also this decrease in the percentage of the dye removed with the temperature raise means that the adsorption process is exothermic.

3.4 Sorption Kinetics:

Pseudo-first order and Pseudo-second order models were employed to analyze the kinetics of SFO adsorption onto Thuja orientalis.

3.4.1 First-order model: the pseudo-first order equation of lagergreen is generally expressed as follows in equation (1)[25]

$$\log (q_1 - q_t) = \log q_1 - \frac{K_1}{2.303} t \text{ ----- (1)}$$

Where q_1 and q_t are the amount of the SFO at adsorbent per unit weight of adsorbent at equilibrium and at time t , respectively (mg/g), and K_1 the rate constant of pseudo-first order sorption (min^{-1}).

The plot of $\log (q_1 - q_t)$ versus t (Figure 7) indicates that such first order expression is not so valid to present system ($R^2 = 0.8216$).

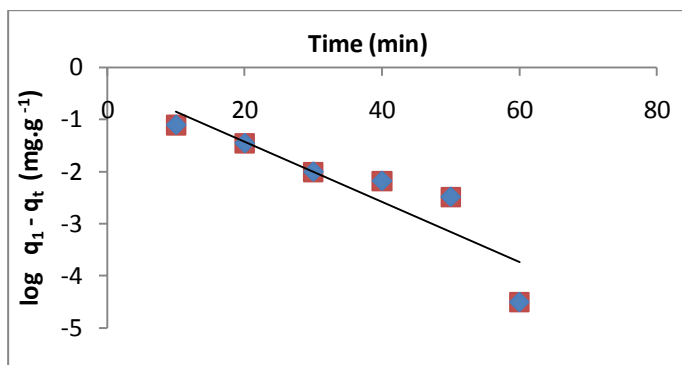


Figure 7- First order plots for adsorption of SFO onto biosorbent.

3.4.2 Second-order model:

The pseudo-second order kinetic rate equation is expressed as [26]:

$$t/q_t = 1/k_2q_2^2 + t/q_2 \dots\dots\dots(2)$$

Where q_2 is the amount of SFO adsorbed at equilibrium (mg, g^{-1}), k_2 is the rate constant of the Pseudo-second-order adsorption ($\text{g, mg}^{-1} \text{min}^{-1}$). The plot of (t/q_t) and t of equation (2) (Figure 8) should give a linear relationship from which q_2 and k_2 can be determined from the slope and intercept of the plot. The pseudo-first order and pseudo-second order sorption constants with the correlation coefficients' R^2 were summarized in Table 1.

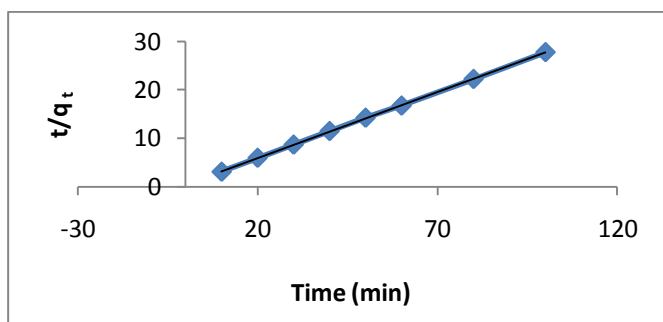


Figure 8- Pseudo-second-order plot for the adsorption of SFO by biosorbent.

Examining fittingness of the models in terms of the R^2 value, it shows that the pseudo-second order kinetic-model describes the system much better than the pseudo-first order kinetic model. The best fit of the pseudo-second order kinetic model in the system shows that chemisorption mechanism involving valence forces through sharing or exchange electron between adsorbent and adsorbate might significantly affect the rate-limiting step [27, 28]. Similar phenomena have been observed in the sorption of SFO onto Fe_2O_3 nanoparticles [29].

Table 1- Pseudo-first and pseudo second-order constants and values of R^2 for SFO adsorption onto Thuja biosorbent.

Pseudo-First order			Pseudo-Secod order		
q_1 . Cal. mg.g^{-1}	K_1 min^{-1}	R^2	q_2 . Cal. g.mg^{-1}	K_2 $\text{g.mg}^{-1}.\text{min}^{-1}$	R^2
0.7655	0.0579	0.8216	3.6617	0.1683	0.9999

3.5 Adsorption isotherms:

In order to successfully represent the equilibrium adsorptive behavior, it is important to have satisfactory description of the equation state between the two phases composing the adsorption system. Four kinds of several isotherm equations were tested to fit experimental data [30]. The Freundlich, Langmuir, Temkin and Dubinin Radushkovich isotherms [31] were applied in this study, these isotherms are useful for comparing results from different sources on a quantitative basis, providing information on the adsorption potential of a material with easily interpretable constants.

3.5.1 Langmuir isotherm:

This model suggested that mono layer adsorption of dye onto a surface containing a finite number of identical binding sites.

The linearized form of this model is given by the equation (3):

$$C_e/q_e = 1/k_L + a/k_L C_e \dots\dots\dots (3)$$

Where C_e is the equilibrium dye concentration (mg, L^{-1}), q_e is the amount adsorbed at equilibrium (mg/g), and (a, k_L) are Langmuir isotherm constants, these parameters can be calculated from the slope and the intercept of the plot of C_e/q_e against C_e , Figure 9 shows the Langmuir isotherm at 283K .

Table 2 lists the parameters calculated. The constants k_L expresses the affinity between the adsorbent and adsorbate. The low value of k_L obtained indicated a high affinity between SFO and Thuja biosorbent.

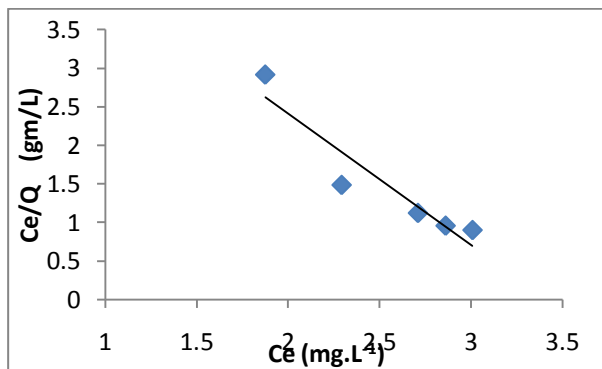


Figure 9- Langmuir's adsorption isotherm plot for the adsorption of SFO onto Thuja biosorbent at 283K.

3.5.2 Freundlich isotherm:

This model assumes that the removal of SFO occurs on a heterogeneous adsorbent surface and can be applied to multilayer adsorption. This isotherm was applied in order to determine the adsorption intensity of the adsorbent for the adsorbate.

The linearized Freundlich isotherm is shown in equation (4):

$$\ln q_e = \ln k_f + \frac{1}{n} \ln C_e \dots\dots\dots (4)$$

The constant k_f is an approximate indicator of adsorption capacity, while $1/n$ is a function of the strength of adsorption in the adsorption process. If $n=1$, then the partition between the two phases are independent of the concentration. If the value of $1/n$ is below one, it indicates a normal adsorption. The linear plot of $\ln q_e$ versus $\ln C_e$ is shown in Figure 10, this enabled determination of the Freundlich constants (k_f, n) from the slope and intercept of the plot. These parameters are shown in Table (2). From the value of the regression coefficient R^2 listed in Table 2 Freundlich isotherm gave a good and better fit to the experiment of data than the Langmuir isotherm.

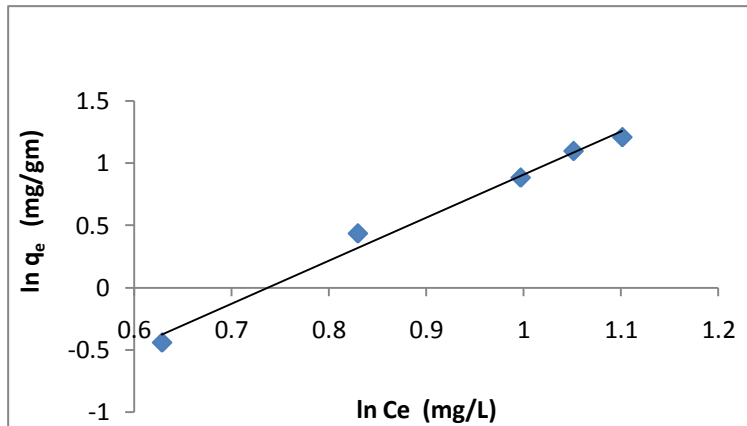


Figure 10- Freundlich adsorption isotherm for the adsorption of SFO onto Thuja biosorbent at 283K.

Table 2- Langmuir, Freundlich, Dubinin Radushkevich and Temkin isotherm modle parameters and their respective correlation coefficients for the sorption of SFO onto Thuja biosorbent.

Temp .K	Langmuir isotherm			Freundlich isotherm					
	K_L (mg.g ⁻¹)	a (L.mg ⁻¹)	R^2	K_f (mg.g ⁻¹)	n	R^2			
283	0.17188	0.2927	0.8868	0.07849	0.28982	0.9886			
293	0.13727	0.29133	0.9070	0.04992	0.26644	0.9954			
303	0.12376	0.26940	0.9087	0.03690	0.26255	0.9777			
313	0.12866	0.2432	0.9541	0.04605	0.29713	0.9834			
T(K)	Temkin isotherm				R^2				
	B	A_T (L/mg)	b_T						
283	5.6319	0.5866	417.76	0.9906					
293	5.9143	0.5499	411.88	0.9696					
303	5.854	0.5174	430.33	0.9492					
313	5.046	0.509	515.712	0.9524					
T(K)	D-R isotherm					R^2	E KJ/mol		
	ϵ^2	B_d mol ² /J ²	K_{D-R} mg/g						
283	1011.03	725.21	546.15	497.43	456.043	-0.00294	2.535	0.9989	13.0412
293	1001.3	690.46	533.84	505.65	480.48	-0.0031	2.6288	0.9892	12.7065
303	974.839	530.418	494.687	488.331	480.499	-0.00299	2.3688	0.920	12.9317
313	993.829	525.668	458.275	450.389	437.582	-0.00351	2.5041	0.9059	11.9332

3.5.3 Temkin isotherm:

This isotherm contains a factor that explicitly taking into account if adsorbent-adsorbate interact and is based on the adsorption that the free energy of adsorption is simply a function of surface coverage.

The linearized Temkin isotherm is shown in equation (5):

$$q_e = B \ln A_T + B \ln C_e \dots\dots\dots(5)$$

Where B equals to = $[RT / b_T]$ In J/mol corresponding to the energy of adsorption, b_T is the Temkin isotherm constant and A_T (L/g) is the equilibrium binding constant related to the maximum binding energy.

Temkin plot of q_e versus $\ln C_e$ at 283K is shown in Figure 11. Both value of B and A_T computed from the slope and intercept of the plot. The Temkin isotherm parameters B, A_T , b_T and R^2 are listed in Table 2. From the value of R^2 this model is applicable to the description of equilibrium data.

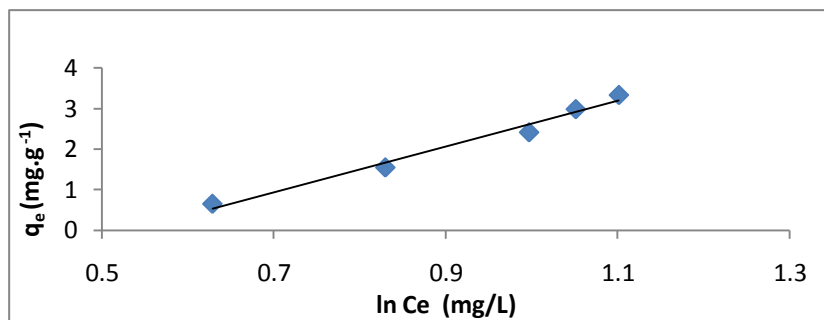


Figure11- Temkin isotherm model on the adsorption of SFO onto biosorbent at 283K.

3.5.4 Dubinin-Radushkevich isotherm D-R:

The D-R isotherm is generally applied to the data in order to deduce the heterogeneity of the surface energies of adsorption and the characteristic porosity of the adsorbent.

The linearized D-R isotherm is shown in equation (6):

$$\ln q_e = \ln k_{D-R} - B_D \varepsilon^2 \dots\dots\dots (6)$$

Where $\varepsilon = RT \ln (1+1/C_e)$ ----- (7)

The value of sorption energy E can be calculated using the equation (8):

$$E = 1 / (2B_D)^{1/2} \dots\dots\dots (8)$$

The D-R constants k_{D-R} in (mg/g) and B_D (mol^2/J^2) representing the theoretical saturation capacity and the mean free energy of adsorption per mol of the adsorbate, R,T and C_e represent the gas constant (8.314 J/ mol.K); absolute temperature (K) and adsorbate equilibrium concentration (mg/L), respectively. The linear plot of the $\ln q_e$ versus ε^2 is shown in Figure 12. The D-K isotherm parameters are given in Table 2.

If the value of E lies between 8 and 16 KJ/mol the sorption process is a chemisorptions one, while values of below 8 KJ/mol indicates a physical adsorption process [32, 33]. The average values of the mean free energy of adsorption (12.635 KJ/mol) obtained indicated chemisorptions between SFO and biosorbent. Also the small values of E indicate that the rate of sorption is relatively fast.

The values of R^2 are regarded as a measure of the goodness-of-fit of experimental data on the isotherm's models. The applicability of the four isotherm's models for the present data approximately follows the order: Freundlich > Temkin > Dubinin Radushkovich > Langmuir.

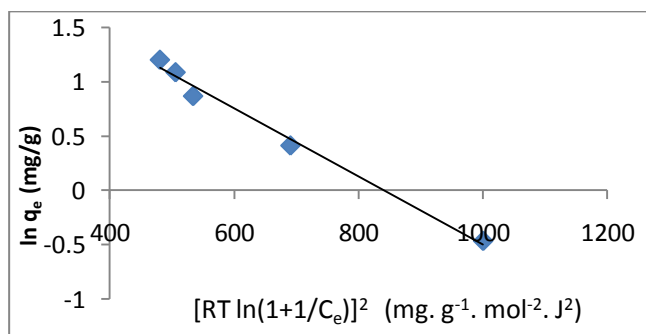


Figure 12- D-R isotherm model for the adsorption of SFO by Thuja biomass.

3.6 Adsorption Thermodynamics:

Analysis of thermodynamics of equilibrium sorption data can give more important information on sorption process. In the present study the effect of temperature on the adsorption course was investigated at different dye concentrations. It showed that the sorption of SFO decrease with increasing the temperature. The decrease in the dye sorption onto Thuja biosorbent is due to the deformation of bonds between the dye molecules and the active site of Thuja biomass. Thermodynamic parameters were calculated using the following equations (9-11) [34]:

$$\Delta G^\circ = - RT \ln k_d \dots\dots\dots(9)$$

Where ΔG° is standard free energy of adsorption, R is the gas constant, k_d is the distribution coefficient for sorption. The k_d value was calculated from the following equation:

$$K_d = C_{Ae} / C_{Se} \dots\dots\dots (10)$$

Where C_{Ac} and C_{Se} are the equilibrium concentrations of dye ions in the adsorbed phase (mg/g) and in the solution (mg/dm^3), respectively. The standard enthalpy (ΔH°) and entropy (ΔS°) of adsorption can be estimated from Van't Hoff equation:

$$\ln k_d = \Delta S^\circ/R - \Delta H^\circ/RT \dots\dots\dots(11)$$

The linear plots of $\ln k_d$ vs. $1/T$ (Figure 13) give the numerical values of enthalpy (ΔH°) and entropy (ΔS°) from the slope and intercept, respectively. The values of the thermodynamic parameters for the sorption of SFO onto biosorbent are given in Table 3. The negative values of the entropy may be indicative of the faster adsorption of the tested dyes onto Thuja biomass, also indicated a decrease in disorderness take place during adsorption process [35]. Degree of spontaneity of the adsorption process is determined by the Gibbs free energy [36]. The negative values of ΔG° for the sorption of SFO onto Thuja biomass are attributed to the spontaneous nature of sorption and it means that the adsorption process is thermodynamically favoured with strong interaction of the dye molecules onto the biosorbent surface. The negative value of enthalpy showed that the adsorption of dye onto adsorbent was exothermic.

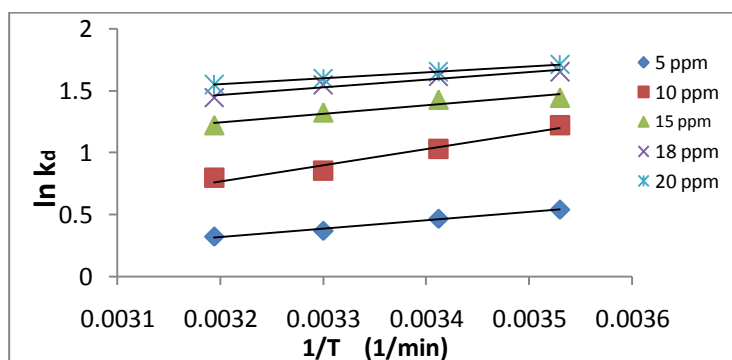


Figure 13- Plot of $1/T$ vs. $\ln k_d$ for the adsorption of SFO onto Thuja biosorbent.

Table 3- Thermodynamic parameters of SFO sorption onto the Thuja biosorbent.

C_o ppm	ΔH° KJ.mol^{-1}	ΔS° J.mol^{-1}	$-\Delta G$ (KJ.mol^{-1})			
			283 K	293 K	303 K	313 K
5	-5.6272	-15.3869	1.2717	1.1348	0.92599	0.83468
10	-10.8340	-28.2800	2.8767	2.5097	2.1534	2.0724
15	-6.8190	-11.5420	3.5170	3.4801	3.3383	3.1799
18	-5.1476	-4.2170	3.8913	3.9381	3.895.3	3.7595
20	-5.0383	-3.0740	4.0349	4.1477	4.1738	4.0302

IV. Conclusion

It could be concluded that Thuja biomass is a potential and cheap biosorbent for removal of SFO from its aqueous solution and industrial wastewater remediation. The sorption kinetics followed the pseudo-second order equation better than pseudo-first order rate model indicating that several processes were involved in dye sorption onto the biosorbent. The equilibrium sorption data are satisfactorily fitted in the order Freundlich > Temkin > Dubinin-Radushkevich > Langmuir. The changes in the standard enthalpy values are found to be negative indicating exothermic process, standard free energy of adsorption was found to be negative which means that the adsorption process is thermodynamically favored.

References

1. Sun, Q. Yang, L. 2003. The adsorption of basic dyes from aqueous solution on modified peat-resin particle, *Water Research*, 37, pp: 1535-1544.
2. Ravi Kumar, M.N.V. Sridhari, T.R. Bhavani, K.D and Dutta, P.K. 1998. Trends in color removal from textile mill effluents. *Colorage*, 40, pp: 25-34.
3. Drabik, M. Touskava, J. Hanns, D. Kobayashi, H. and Biederman, H. 2010. Properties of composite films of titania nanofibers and safranin o dye. *Synthetic metals*, 160, pp: 2564-2572.

4. Al-Bastaki, N. Banat, F. **2004**. Combining ultrafiltration and adsorption on bentonite in a one-step process for the treatment of colored waters. *Resource conservation & Recycling*, 41, pp:103-133.
5. Golder, A.K. Hridaya, N. Samanta, A.N. Ray, S. **2005**. Electrocoagulation of methylene blue and eosin yellowish using mild steel electrode. *Journal of Hazardous materials*, 127, pp: 134-140.
6. Forgacs, E. Cserhati, T. Oros, G. **2004**. Removal of synthetic dyes from wastewater ;a review. *Environment international*, 30, pp: 953-971.
7. Chatterjee, S. . Lee, D. Lee, M.W. Woo, S. H. **2009**. Enhanced adsorption of congo red from aqueous solutions by chitosan hydrogel beads impregnated with acetyl trimethyl ammonium bromide. *Bioresource technology*, 100, pp: 2803-2809.
8. Yener, J. Turkan, K. ; Dogu G. and Dogu, T. **2006**. Adsorption of basic yellow 28 from aqueous solutions with clinoptilolite and amberlite. *Journal of colloid and Interface science*, 294(2), pp: 255-264.
9. Aksu, Z. **2005**. Application of adsorption for the removal of organic pollutants. *Process Biochemistry*. 40(3-4) , pp: 997-1026.
10. HO, Y.S. Ching T.H. and Hsueh, Y.M. **2005**. Y.M. Removal of basic dye from aqueous solution using tree fern as bio adsorption. *Process Biochemistry*, 40(1), pp:119-124.
11. Arawi, M. Yousefi, L.N. Mahaoodi, N.M. Niyaz M. and Tabrizi, N. S. **2005**. Removal of dyes from colored textile waste water by orange pet adsorbent: equilibrium and kinetic studies. *Journal of colloid and Interface science*, 288(2), pp:371-376.
12. Banat, F. Al- Asheh S. and Al- Makhadmen L. **2003**. Evaluation of the use of raw and activated date pits as potential adsorbents for dye containing waters. *Process Biochemistry*, 39(2), pp: 193-202.
13. Gong, R. Sun, Y. Cheu, J. Lin, H. and Yang, C. **2005**. Effect of chemical modification on dye adsorption capacity of peanut hull. *Dyes and pigments*, 67(3), pp: 175-181.
14. Han, R. Zon, W. Yu, W. Cheng, S. Wang, Y. Shi, J. **2007**. Biosorption of methylene blue from aqueous solution by fallen phoenix trees leaves. *Journal of Hazardous materials*, 141 , pp: 156-162.
15. El-Sayed, G. O. **2011**. Removal of methylene blue and crystal violet from aqueous solutions by palm kerned fiber. *Desalination*, 272, pp: 225-232.
16. Gupta, V. K. Mittal, A. Jain, R. Mathur M. and Sikarwar ,S. **2006**. Adsorption of safranin T from waste water using waste material activated carbon and activated rice husks. *Journal of colloid and Interface Science*, 303(3), pp: 80-86.
17. Zaghbani, N. Hafianc A. and Dhahbi, M. **2008**. Removal of Safranin T from waste water using micellar enhanced ultrafiltration. *Desalination*, 222, pp: 348-356.
18. Nuhoglu, Y. . Oguz, E. **2003**. Removal of copper (II) from aqueous solutions by biosorption on the cone biomass of thuja orientalis. *Process Biochemistry*, 34, pp: 1627-1631.
19. Kavitha , D. Namasivayam, C. **2007**, Experimental and kinetic studies one methylene blue adsorption by coir pith carbon. *Bioresour Technology*, (98), pp: 14-21.
20. Al-Mammar, D.E. **2013**, Removal of brilliant green dye from aqueous solution by adsorption onto modified clay. *Ibn AL-Haitham Journal for Pure and Applied Science*, 26(2), pp: 206-219.
21. Annadurai, G. Juang R.S. and Lee, D. J. **2002**. use of cellulose-based wastes for adsorption of dyes from aqueous solutions. *Journal of Hazardous materials*, B92, pp: 263-274.
22. Alam, M. Nadem R. and Jilani, M. I. **2012**. Pb (II) removal from waste water using pomegranate waste biomass. *International Journal of chemical and Biochemical sciences*, 1, pp: 24-29.
23. Srivatava, V. C. . Mall I. D and I. Mishra, M. **2006**. Equilibrium modeling of single and binary adsorption of cadmium and nickel on to baggase fly ash. *Journal of Chemical Engineering*, 117, pp: 79-91.
24. Ho Y.S. and Chiang, C. C. **2001**. Sorption Studies of acid dye by mixed sorbent. *Adsorption Journal of International Adsorption Society* , 7, pp:139-147 .
25. Arunachalam ,R. and Annadurai, G. **2011**. Nano-porous adsorbent from fruit peel waste for Decolorization studies. *Research Journal of Environmental science*, 5(4), pp: 366-376.
26. Yeddon N. and Bensaili. A. **2005**. Kinetic models for the sorption of dye from aqueous solution by clay-wood sawdust mixture. *Desalination*, 185, pp: 499-508.
27. Bulut, y. , Tiz , Z. **2007** . Removal of heavy metals from aqueous solution by sawdust adsorption. *Journal of Environmental Science*, 19, pp: 160-166.

28. Ngah, w.s. Ab Ghani, S., kamari, A. **2005**. Adsorption behavior of Fe (II) and Fe (III) ions in aqueous solution on chitosan and cross-linked chitosan beads. *Bioresource Technology*, 96, pp: 443-450.
29. Shariati,S. Faraji,M. Yamini Y. and A-Rajabi, A.**2011**. Fe₂O₃ magnetic nanoparticles modified with sodium dodecyl sulfate for removal of safranin O dye from aqueous solutions. *Desalination*, 270, pp: 160-165 .
30. El-Ashtoukhy,E. S. Z. Amin N. K. and Abdelwahab, O.**2008**. Removal of lead (II) and copper (II) from aqueous solution using pomegranate pell as anew adsorbent. *Desalination*, 223, pp: 162-173 .
31. Jayaraj,R. Thanaraj, P. J. Natarajan S. T. and Prasath,P. M. D.**2011**. Removal of congo red dye from aqueous solution using acid activated ecofriendly low-cost carbon prepared from marine alagae voloria bryopsis. *Journal of Chemical and Pharmaceutical Research*, 3 (3), pp:389-396.
32. Sivakumar, P. and Palanisamy,P. N. **2009**.Adsorption studies of basic red 29 by a non conventional activated carbon prepared from euphorbia antiqorum L. *International Journal of Chemical Technology Research*, 1(3), pp:502-510 .
33. Dada, A. O, Olalekam, A.P, Olatunya, A.M., Dada, O.**2012**. Laugmuir, Freundlich, Temkim and Dubinin-Radushkevish isotherms studies of equilibrium sorption of Zn⁺² unto phosphoric acid modified rice husk. *IOSR Journal of Applied Chemistry*, 3(1), pp: 38-45.
34. Chosh, D. and Bhattacharyya,K. G. **2002**. Adsorption of methylene blue on kaolinite .*Applied Clay Science*, 20, pp: 295-300.
35. Rafiquee, M Saxena,N. Khan S. and Quraishi,M. **2007**. Some fatty acid oxadiazoles for corrosion inhibition of mild steel in HCl. *Indian Journal of Chemical Technology*, 14, pp: 576-583.
36. Bouklah, M. Itammouti,B.**2006**. Thermodynamic characterization of steel corrosion for the corrosion inhibition of steel in sulphuric acid solutions by Artemisia. *Portugaliae Electrochemical Acta*, 24, pp: 457-468.